Available online at www.sciencedirect.com
SCIENCE DIRECT
Journal of Power Sources 146 (2005) 516–520
JOURNAL OF POWER SOURCES
www.elsevier.com/locate/jpowsour

Structural and electrochemical properties of lithium vanadium fluorophosphate, $LiVPO_4F$

J. Barker [a,*], R.K.B. Gover [a], P. Burns [a], A. Bryan [a], M.Y. Saidi [b], J.L. Swoyer [b]

[a] *Valence Technology Inc., Unit 62, Rissington Business Park, Gloucestershire, GL54 2QB, UK*
[b] *Valence Technology Inc., 301 Conestoga Way, Henderson, NV 89015, USA*

Available online 31 May 2005

Abstract

The electroactive lithium vanadium fluorophosphate phase, $LiVPO_4F$ ($P\bar{1}$, $a = 5.1687(2)$ Å, $b = 5.3062(2)$ Å, $c = 7.5031(3)$ Å, $\alpha = 66.856(2)^\circ$, $\beta = 67.004(2)^\circ$, $\gamma = 81.583(2)^\circ$ and cell volume = 174.21(1) Å^3) has been synthesized by a two-step reaction scheme based on a carbothermal reduction (CTR) process. High-resolution electrochemical measurements reveal a structured voltage response for the lithium extraction process while the lithium insertion process proceeds via a two-phase reaction mechanism centered at around 4.2 V versus Li. Performance evaluation of a graphite||$LiVPO_4F$ lithium-ion cell indicates an average discharge voltage of 4.06 V coupled to an initial material utilization for the $LiVPO_4F$ of around 123 mAh g^{-1}. Long-term cycling of this lithium-ion system demonstrates good capacity retention over the first 300 cycles. Based on the available data we believe the $LiVPO_4F$ offers considerable promise as a viable cathode replacement for $LiCoO_2$.

Keywords: Lithium; Vanadium; Fluorophosphate; Insertion

1. Introduction

Framework phosphate materials such as $LiFePO_4$ [1] and $Li_3V_2(PO_4)_3$ [2] have been identified as potential electroactive materials for lithium ion battery applications. We recently reported the preliminary electrochemical evaluation of a series of novel fluorophosphate phases represented by the general formula $LiMPO_4F$, where M represents a 3d transition metal [3–5]. Of particular interest is the effect of structural fluorine on the insertion properties of these polyanion compounds [5]. In general the occurrence of fluorophosphate phases is considered quite rare, although a few examples have been reported previously [6]. Related compounds include $KAlPO_4F$ [7], NH_4FePO_4F [8] and $Na_3M_2(PO_4)_2F_3$ (where M = Al, V, Cr, Fe, Ga) [9], as well as the known minerals lacroixite $NaAlPO_4F$ [10], montebrasite $LiAl(PO_4)(OH,F)$ [10] and ambylgonite $(Li,Na)AlPO_4(OH,F)$ [11]. X-ray diffraction studies indicate that the $LiMPO_4F$ compounds are iso-structural with the naturally occurring mineral tavorite, $LiFePO_4{\cdot}OH$, crystallizing with a triclinic structure (space group $P\bar{1}$) [3,4]. In this communication we report on the electrochemical performance characteristics of a representative compound from this general series, the lithium vanadium fluorophosphate, $LiVPO_4F$. In particular we evaluate the properties of this phase in a lithium-ion configuration, where it is capacity matched with a crystalline graphite anode material.

2. Experimental

The $LiVPO_4F$ samples used in this study were all prepared using the carbothermal reduction (CTR) method [12,13] using VPO_4 as a reaction intermediate. The precise CTR reaction conditions for the VPO_4 preparation were determined by a semi-empirical approach based on the thermodynamic (free energy–temperature relation) requirements for a V^{5+} to V^{3+} transition [13]. Since these reductive conditions were found to favor the C → CO carbothermal reaction mechanism, the VPO_4 preparative reaction scheme may be summarized:

$$0.5\,V_2O_5 + (NH_4)_2HPO_4 + C \rightarrow VPO_4 + 2.0\,NH_3 + 1.5\,H_2O + CO \quad (1)$$

* Corresponding author.
E-mail address: jerry.barker@valence.com (J. Barker).

0378-7753/$ – see front matter © 2005 Elsevier B.V. All rights reserved.
doi:10.1016/j.jpowsour.2005.03.126

The precursors – V_2O_5 (Alfa-Aesar), $(NH_4)_2HPO_4$ (Alfa-Aesar) and high surface area carbon – were intimately mixed and then pelletized. To ensure complete vanadium reduction and the presence of residual carbon in the product phase, a 50% mass excess of carbon was used over the stoichiometric conditions represented on reaction (1) above. The precursor mixture was heated to an ultimate reaction temperature of between 700 and 800 °C and held for between 8 and 16 h inside a temperature controlled tube furnace (Carbolite Ltd., England). The CTR VPO_4 product, which was predominantly black in color (consistent with the presence of residual carbon black), was then further reacted with LiF (Alfa-Aesar) at 700–850 °C to yield the single phase $LiVPO_4F$ product:

$$LiF + VPO_4 \rightarrow LiVPO_4F \quad (2)$$

Structural and crystallographic analyses of the VPO_4 and $LiVPO_4F$ were based on powder diffraction data obtained using a Siemens D5000 X-ray diffractometer (in Bragg-Bretano geometry) equipped with Cu Kα radiation. Structure analysis using the Rietveld method was performed using the GSAS software package [14–16]. Electrochemical evaluation of the test materials was carried out in metallic lithium (FMC) test cells using a commercial (Maccor Inc.) battery cycler. For lithium-ion cell testing the $LiVPO_4F$ was capacity matched with a low surface area crystalline graphite. Typical cathode loadings were in the range 10–20 mg cm^{-2} and an electrode diameter of 20 mm was used throughout. The positive electrodes comprised 84 wt% active materials, 5 wt.% Super P (conductive carbon) and 11 wt.% PVdF-HFP co-polymer (Elf Atochem) binder. The electrolyte was composed of a 1 M $LiPF_6$ solution in ethylene carbonate/dimethyl carbonate (2:1 by weight) and the electrode separator comprised a dried glass fiber filter (Whatman, Grade GF/A). High-resolution electrochemical measurements were performed using the Electrochemical Voltage Spectroscopy (EVS) technique [17].

3. Structure

X-ray diffraction data for the reaction intermediate CTR VPO_4 were comparable with those reported elsewhere for the material made by conventional solid-state synthesis methods [18–20]. Structural refinement generated the following crystallographic parameters—$a = 5.2323(5)$ Å, $b = 7.7760(2)$ Å, $c = 6.2831(5)$ Å and cell volume = 255.64(4) $Å^3$. VPO_4 is isostructural with $CrVO_4$, (orthorhombic space group *Cmcm*), and comprises chains of edge sharing VO_6 octahedra, which are linked by PO_4 tetrahedra [20].

Fig. 1 shows the fit obtained from Rietveld refinement for a typical sample of CTR prepared $LiVPO_4F$. As expected no diffraction peaks were identifiable as LiF, an observation that confirmed complete LiF incorporation. This incorporation reaction results in a loss of crystal symmetry such that the $LiVPO_4F$ product phase adopts a triclinic

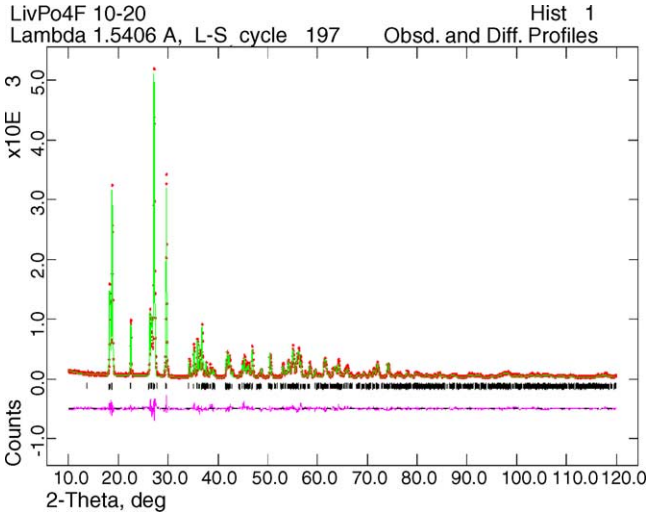

Fig. 1. Observed, calculated and difference plots obtained for $LiVPO_4F$ from Rietveld refinement. The diffraction patterns were refined based on a triclinic structure using space group $P\bar{1}$ (see text for unit cell parameters).

structure (space group $P\bar{1}$). A structural model was successfully refined based on a triclinic structure using space group *P*-1: $a = 5.1687(2)$ Å, $b = 5.3062(2)$ Å, $c = 7.5031(3)$ Å, $\alpha = 66.856(2)$, $\beta = 67.004(2)$, $\gamma = 81.583(2)$ and cell volume = 174.21(1) $Å^3$. The $LiVPO_4F$ structure comprises a three dimensional framework built up from PO_4 tetrahedra and VO_4F_2 octahedra [3]. Fig. 2 shows a representation (shown along the *c* axis) of the $LiVPO_4F$ structure.

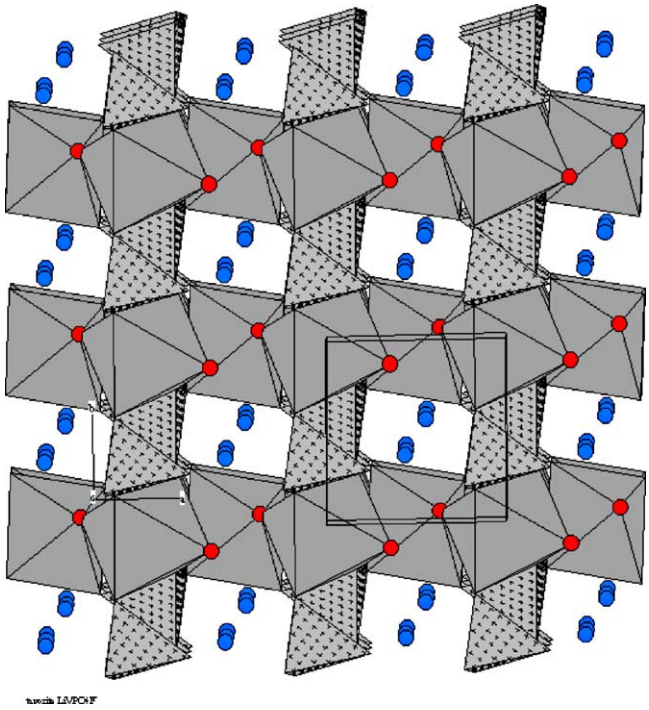

Fig. 2. Schematic representation of the $LiVPO_4F$ framework structure (shown in the *c* direction) indicating the position of the Li^+ ions.

4. Electrochemical behavior

The lithium extraction/insertion behavior for the $LiVPO_4F$ active material relies on the reversibility of the V^{3+}/V^{4+} redox couple:

$$LiV^{3+}PO_4F \leftrightarrow V^{4+}PO_4F + Li^+ + e^- \quad (3)$$

Fig. 3 shows the EVS first cycle data for a representative Li||$LiVPO_4F$ cell. The reversible specific capacity is close to the theoretical material utilization of 155 mAh g^{-1}, and there is a low level of voltage polarization. This performance is a significant improvement over our previous publication [3,4] and results from the optimized preparative conditions employed. The end of the charge process represents formation of the fully delithiated VPO_4F phase. Transition metal fluorophosphate phases are highly unusual and we are currently determining the crystallographic properties of the vanadium (IV) fluorophosphate phase [21]. Close inspection of this figure indicates the presence of a small inflection in the charge voltage profile. This behavior is best depicted in the differential capacity data, which reveals the presence of two closely spaced peaks during cell charge. This observation corresponds to extraction of the alkali ions from two (energetically inequivalent) crystallographic sites within the $LiVPO_4F$ framework. By contrast, the subsequent lithium insertion process is characterized by a single differential capacity peak, consistent with a two-phase reaction mechanism [1]. In situ X-ray studies are currently underway in our laboratory to elucidate the precise nature of this lithium extraction/insertion sequence [21]. The electrochemical response recorded during this initial EVS cycle, persists over several 100 cycles and may be considered characteristic of the lithium insertion reactions.

In Fig. 4 we compare the voltage profiles of graphite||$LiVPO_4F$ and graphite||$LiCoO_2$ lithium-ion cells made using identical anode stock and employing similar electrode mass balances. The reversible specific capacities of the two active materials were determined to be similar, i.e., 129 and 132 mAh g^{-1} for the $LiVPO_4F$ and $LiCoO_2$, respectively. By inspection we may also determine that the $LiVPO_4F$ cell offers not only a flatter voltage profile but also generates an average discharge voltage around 0.3 V higher than the comparable $LiCoO_2$ system. In addition to electrochemical performance, safety considerations will also be of paramount importance in establishing if $LiVPO_4F$ will be commercially viable, especially for larger format applications. Based on structural and M–O–P bonding considerations, we would expect the fluorophosphates to behave similarly to $Li_3V_2(PO_4)_3$ and $LiFePO_4$ and represent a substantially safer cathode option than $LiCoO_2$ or other oxide based active materials [1–3]. Comprehensive testing is currently underway to define and confirm these safety characteristics [21].

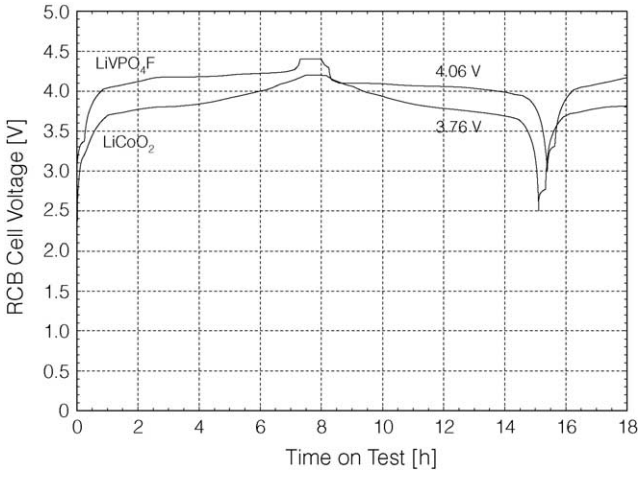

Fig. 4. Comparative voltage profiles for graphite||$LiVPO_4F$ and graphite||$LiCoO_2$ lithium-ion cells. The data were collected at approximate charge/discharge rate of C/8. The electrolyte in both iterations comprised a 1 M $LiPF_6$ solution in ethylene carbonate/dimethyl carbonate (2:1 by weight).

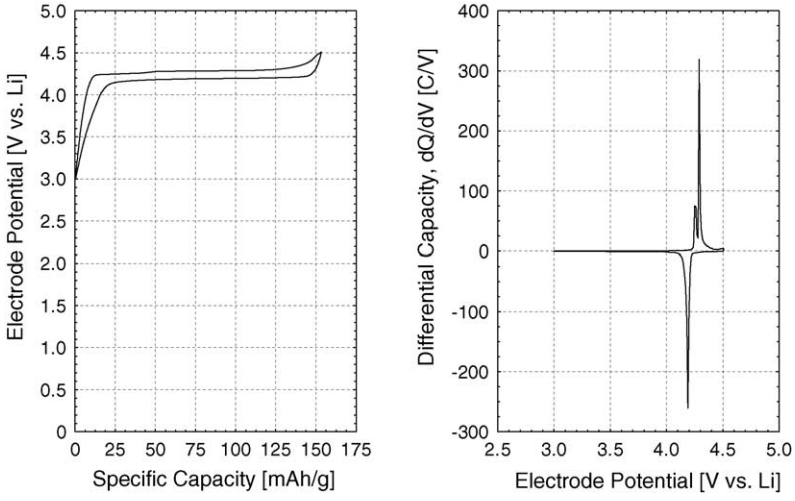

Fig. 3. EVS data for a typical Li||$LiVPO_4F$ cell cycled between 3.00 and 4.50 V. The data shown were collected at 23 °C and are for the first cycle. The electrolyte comprised a 1 M $LiPF_6$ solution in ethylene carbonate/dimethyl carbonate (2:1 by weight). Left: EVS voltage profile. Right: EVS differential capacity profile.

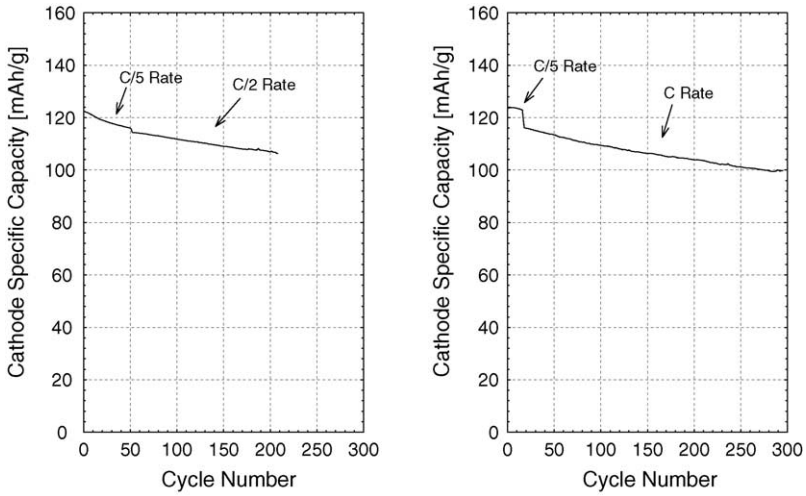

Fig. 5. Lifetime cycling of representative graphite||$LiVPO_4F$ lithium-ion cells cycled between 3.00 and 4.40 V. The data shown were collected at 23 °C using an electrolyte that comprised a 1 M $LiPF_6$ solution in ethylene carbonate/dimethyl carbonate (2:1 by weight). Left: C/2 rate for charge/discharge. Right: C rate for charge/discharge. Note that these cells were initially tested at C/5 rate and then switched to higher rates as shown by the step in the data and the text annotation.

In Fig. 5 we demonstrate the long-term stability of the graphite||$LiVPO_4F$ lithium ion system by cycling representative test cells at charge/discharge rates of C/2 and C. As indicated on this figure the initial cycling was carried out at a C/5 rate. From inspection we may conclude that there is a relatively insignificant discharge capacity 'penalty' when increasing the rate from C/5 to C. For instance, the initial reversible specific capacity for the active material is around 125 mAh g^{-1} at C/5 and this figure declines to about 117 mAh g^{-1} when the rate in increased to the C rate. Following the first three cycles, the charge/discharge efficiencies for the data shown in Fig. 5 are found to be close to 100%. In addition, the presented cycling results suggest that the rate capability of the fluorophosphate is superior to other polyanion active materials such as $LiMPO_4$ (M = Fe, Mn) [1] or $LiVOPO_4$ [22]. To support this position, some preliminary test data confirm that the electronic conductivity and Li ion diffusion rates for $LiVPO_4F$ are both significantly higher than in either $LiFePO_4$ or $LiVOPO_4$ [21].

The cycling performance confirms that the $LiVPO_4$ offers good long-term stability with comparatively low capacity fade characteristics. This type of cycling behavior is comparable to similar lithium-ion testing using commercial $LiCoO_2$ [23]. High-resolution EVS experiments carried out on lithium-ion cells cycled more than 150 times (not shown here) indicate insignificant changes in the voltage-capacity and differential capacity responses. In addition, ex situ diffraction studies demonstrate minor structural differences between cycled and pristine electrodes [21].

5. Conclusions

Despite the commercial success of $LiCoO_2$-based lithium-ion batteries, there is still a continual requirement for electroactive materials with improved electrochemical and safety properties. In this communication we demonstrate the performance characteristics of the novel fluorophosphate phase, $LiVPO_4F$. In lithium metal test cells the $LiVPO_4F$ demonstrates a reversible specific capacity of around 140 mAh g^{-1} and an average discharge (insertion) voltage of 4.2 V versus Li. In addition, the active material shows good capacity retention during long-term cycling tests in graphite-based lithium-ion systems. In terms of rate capability the performance appears superior to the $LiMPO_4$ (M = Fe, Mn) polyanion materials [1]. By comparison with lithium-ion cells based on the established material $LiCoO_2$, the fluorophosphate material offers an improved voltage profile and a higher average discharge voltage. The material is also fully compatible with existing lithium-ion cell 'infrastructure' such as electrolyte formulations and charge circuit electronics. In summary, we believe that based on these preliminary performance data the $LiVPO_4F$ offers considerable promise as a viable cathode replacement for $LiCoO_2$.

References

[1] A.K. Padhi, K.S. Nanjundaswamy, C. Masquelier, J.B. Goodenough, J. Electrochem. Soc. 144 (1997) 2581.
[2] (a) J. Barker, M.Y. Saidi, US Patent 5,871,866. Filed September 1996, issued February 1999;
(b) M.Y. Saidi, J. Barker, H. Huang, J.L. Swoyer, G. Adamson, Electrochem. Solid State Lett. 5 (2002) A149.
[3] J. Barker, M.Y. Saidi, J. Swoyer, US Patent 6,387,568. Filed April 2000, issued May 2002.
[4] J. Barker, M.Y. Saidi, J. Swoyer, J. Electrochem. Soc. 150 (2003) A1394.
[5] J. Barker, M.Y. Saidi, J. Swoyer, J. Electrochem. Soc. 151 (2004) A1670.
[6] M.T. Averbuch-Pouchot, A. Durif, Topics in Phosphate Chemistry, World Scientific Press, Singapore, 1996, p. 108.

[7] S.J. Kirkby, A.J. Lough, G.A. Ozin, Z. Kristallogr. 2 (1995) 956.
[8] Th. Loiseau, Y. Calage, P. Lacorre, G. Ferey, J. Solid State Chem. 111 (1994) 390.
[9] J.-M. Le Meins, M.-P. Cronier-Lopez, A. Hemon-Ribaud, G. Courbion, J. Solid State Chem. 148 (1999) 260.
[10] L.A. Groat, B.C. Chakoumakos, D.H. Brouwer, C.M. Hoffman, C.A. Fyfe, H. Morell, A.J. Schultz, Am. Miner. 88 (2003) 195.
[11] A.A. Moss, E.E. Fejer, P.G. Embrey, Miner. Magn. 37 (1969) 414.
[12] H.T. Ellingham, J. Soc. Chem. Ind. 63 (1944) 125.
[13] J.D. Gilchrist, Extraction Metallurgy, 2nd ed., Pergamon Press, Oxford, 1980, p. 161.
[14] H.M. Rietveld, J. Appl. Crystallogr. 2 (1969) 65.
[15] R.A. Young (Ed.), The Rietveld Method, Oxford University Press, New York, 1993.
[16] A.C. Larsen, R.B. Von Dreele, Los Alamos Laboratory Report, NO-LA-U-86-746, 1987.
[17] J. Barker, Electrochim. Acta 40 (1995) 1603.
[18] N. Kinomura, F. Muto, M. Koizumi, J. Solid State Chem. 45 (1982) 252.
[19] T. Yamauchi, Y. Ueda, J. Magn. Magn. Mater. 705 (1998) 177–181.
[20] E.J. Baran, J. Mater. Sci. 33 (1998) 2479.
[21] J. Barker, R.K.B. Gover, P. Burns, A. Bryan, J. Electrochem. Soc., in press, 2005.
[22] N. Dupre, J. Gaubicher, T. Le Mercier, G. Wallez, J. Angenault, M. Quarton, Solid State Ionics 140 (2001) 209.
[23] R. Koksbang, J. Barker, H. Shi, M.Y. Saidi, Solid State Ionics 84 (1996) 1.